https://doi.org/10.30799/jnst.S201.26110301 J. Nanosci. Tech. - Volume 11 Issue 3 (2026) 1078–1081

Share Your Innovations through JACS Directory

Journal of Nanoscience and Technology

Visit Journal at https://www.jacsdirectory.com/jnst

ISSN: 2455-0191

Synthesis and Characterization of CuO–CdS Nanocomposites for Photodegradation Applications

Gokul V. Suryawanshi*, Tulshidas S. Savale

Dept. of Chemistry, M.G.V's M.S.G. Arts, Science and Commerce College, Malegaon Camp, Malegaon, Nashik – 423 105, Maharashtra, India.

ARTICLEDETAILS

Article history:
Received 24 February 2026
Accepted 11 March 2026
Available online 15 April 2026

Keywords:
Nanocomposite
CuO-CdS
Chemical Precipitation Method

ABSTRACT

In the present work, a 0.5 at% CuO–CdS nanocomposite was successfully synthesized using a facile chemical method and systematically investigated for its structural, morphological, optical, and photocatalytic properties. X-ray diffraction (XRD) analysis confirmed the coexistence of hexagonal CdS and monoclinic CuO phases without the formation of secondary impurities, indicating successful heterostructure formation. Field emission scanning electron microscopy (FESEM) revealed significant morphological modification in the composite, exhibiting hierarchical flower-like and rod-shaped nanostructures with enhanced surface roughness. Energy dispersive X-ray (EDX) analysis verified the presence of Cu, Cd, S, and O elements, confirming phase purity, while FT-IR spectroscopy confirmed the formation of characteristic Cu–O and Cd–S bonds along with surface hydroxyl groups. UV–visible absorption studies demonstrated enhanced visible-light absorption and a slight red shift in the CuO–CdS nanocomposite compared to pure CdS, indicating improved light harvesting ability. Photoluminescence (PL) analysis showed significant quenching of emission intensity in the composite, suggesting efficient suppression of electron–hole recombination due to effective charge separation at the CuO/CdS interface. The photocatalytic activity of the synthesized nanocomposite was evaluated through the degradation of methylene blue (MB) dye under UV–Visible irradiation. The CuO–CdS heterostructure exhibited superior degradation efficiency compared to individual components, attributed to enhanced charge transfer and the generation of reactive oxygen species. The results demonstrate that the CuO–CdS nanocomposite is a promising material for visible-light-driven photocatalytic applications and wastewater treatment.

1. Introduction

Nanoparticles, both metallic and non-metallic, have a wide range of applications. Metal nanoparticles have many applications in physics, chemistry, materials science and industry [1-3]. Semiconducting metal oxides such as CuO, In_2O_3, TiO_2, NiO and ZnO and their compounds with carbon-based materials such as carbon nanotubes, graphene oxide, graphene and heterostructures (n-type and p-type semiconductors) are being investigated for their technological importance. characteristics Copper oxide (CuO) is used in many applications, including gas sensors. [4]. Nanoparticles have attractive properties that differ significantly from their bulk state [5]. Gas-sensitive metal oxide semiconductors are amazing because their morphological and structural content can be changed to improve sensitivity [6-8].

Water contamination by synthetic dyes is a major environmental concern due to rapid industrial expansion, particularly in textile, paper, leather, and pharmaceutical industries. Among various organic dyes, methylene blue (MB) is widely used and frequently detected in industrial effluents. Although MB is less toxic compared to some azo dyes, its high stability, intense color, and resistance to biodegradation can cause serious ecological imbalance by reducing light penetration in aquatic systems and affecting photosynthetic activity [9]. Therefore, efficient removal of MB from wastewater is of significant environmental importance.

Conventional treatment techniques such as adsorption, coagulation, membrane filtration, and biological degradation often suffer from limitations including incomplete degradation, sludge generation, and secondary pollution [10]. In this context, semiconductor-based photocatalytic degradation has emerged as a promising green technology for the mineralization of organic dyes into harmless end products such as CO_2 and H_2O under light irradiation [11].

Photocatalytic degradation of MB involves the excitation of a semiconductor catalyst under visible or UV light, leading to the generation of electron–hole pairs. These charge carriers react with surface-adsorbed oxygen and water molecules to produce highly reactive oxygen species (ROS), such as hydroxyl radicals ($^{\bullet}OH$) and superoxide radicals ($O_2^{\bullet-}$), which oxidatively decompose the dye molecules [12]. Among visible-light-responsive semiconductors, CdS has attracted considerable attention due to its narrow band gap (~2.4 eV) and strong absorption in the visible region [12]. However, the practical application of CdS is hindered by rapid recombination of photogenerated charge carriers and photocorrosion under light irradiation [13].

CuO, a p-type semiconductor with a narrow band gap (~1.2–1.5 eV), exhibits good chemical stability and visible light absorption capability, making it suitable for dye degradation applications [13]. Nevertheless, pure CuO also suffers from limited photocatalytic efficiency due to insufficient charge separation. To overcome these drawbacks, the construction of CuO–CdS heterojunction nanocomposites has proven to be an effective strategy. The formation of a p–n heterojunction between CuO and CdS enhances interfacial charge transfer, suppresses electron–hole recombination, and significantly improves the photodegradation efficiency of MB under visible light irradiation [14].

Thus, the work on CuO–CdS nanocomposites has been done for a promising photocatalytic system for efficient and sustainable removal of methylene blue from contaminated water.

2. Experimental Methods

2.1 Synthesis of CuO-NPs

CuO nanoparticles were synthesized via a conventional chemical precipitation (deposition) method. In a typical procedure, 4 g of copper(II) chloride dihydrate ($CuCl_2 \cdot 2H_2O$) was dissolved in 150 mL of ethanol under continuous stirring to obtain a homogeneous precursor solution. Separately, 2 g of sodium hydroxide (NaOH) pellets were dissolved in 50 mL of ethanol to prepare the alkaline solution.

*Corresponding Author:gklsuryawanshi24@gmail.com(Gokul V. Suryawanshi)

https://doi.org/10.30799/jnst.S201.26110301

The NaOH solution was added dropwise to the copper precursor solution at room temperature under constant magnetic stirring to ensure uniform mixing and controlled nucleation. During the course of the reaction, the solution underwent a distinct color transition from green to bluish-green and finally to black, indicating the formation of copper hydroxide as an intermediate precipitate. The resulting dark precipitate was collected by centrifugation and thoroughly washed several times with ethanol followed by deionized water to eliminate residual sodium and chloride ions. The purified precipitate was then dried in a desiccator at approximately 50 °C to remove moisture content.

Subsequently, the dried material was subjected to thermal treatment (annealing) at different temperatures, 200 °C, 300 °C, and 400 °C, to promote phase transformation and improve crystallinity. After annealing, the obtained material was gently ground into fine powder to yield CuO nanoparticles suitable for further characterization studies.

2.2 Synthesis of CdS-NPs

Cadmium sulfide (CdS) nanoparticles were prepared using a facile and cost-effective aqueous precipitation method. In this process, cadmium nitrate was employed as the cadmium source, while sodium sulfide served as the sulfide precursor. Owing to the extremely low solubility of CdS in water, the reaction between these two aqueous solutions leads to the immediate formation of a solid precipitate through a metathesis reaction.

Typically, an aqueous solution of cadmium nitrate was prepared under continuous stirring, followed by the gradual addition of sodium sulfide solution. Upon mixing, a yellow precipitate corresponding to CdS was formed, indicating successful nucleation and growth of nanoparticles. The precipitation reaction can be represented as:

$$Cd(NO_3)_{2\,(aq)} + Na_2S_{\,(aq)} \rightarrow CdS_{\,(s)}\downarrow + 2NaNO_{3\,(aq)}$$

To regulate particle growth and prevent agglomeration, a small quantity of diethylene glycol was introduced as a stabilizing (capping) agent. The presence of diethylene glycol helps control the nucleation process and restrict particle aggregation by providing steric stabilization, thereby enabling better control over nanoparticle size distribution.

The resulting CdS precipitate was separated, washed thoroughly with deionized water to remove soluble by-products, and subsequently dried to obtain fine CdS nanopowder suitable for further characterization and application studies.

2.3 Synthesis of CuO-CdS Nanocomposites

CuO–CdS nanocomposites were synthesized by a simple sol–gel method using stoichiometric quantities of metal precursors. In a typical procedure, 2.0 g of copper(II) chloride dihydrate ($CuCl_2{\cdot}2H_2O$) was dissolved in 100 mL of ethanol under continuous magnetic stirring to obtain a clear solution. Separately, 1.5 g of cadmium nitrate tetrahydrate ($Cd(NO_3)_2{\cdot}4H_2O$) was dissolved in 50 mL of distilled water, followed by the addition of 0.8 g of sodium sulfide (Na_2S) to form a CdS sol under constant stirring. The CdS sol was added dropwise to the copper precursor solution while stirring continuously at room temperature. The mixture was stirred for 3–4 hours to ensure uniform mixing and gel formation. A small quantity (approximately 5 mL) of diethylene glycol was added as a stabilizing agent to control particle growth and prevent agglomeration.

The resulting gel was aged for 12 hours, followed by drying at 70 °C to obtain a xerogel. The dried material was then calcined at 300 °C for 2 hours to promote crystallization and formation of the CuO–CdS nanocomposite. Finally, the annealed product was ground gently to obtain fine nanocomposite powder for further characterization.

3. Results and Discussion

3.1 X-Ray Diffraction Analysis

The X-ray diffraction (XRD) patterns of pure CdS, CuO, and 0.5 at% CuO–CdS nanocomposite are shown in the Fig. 1. The XRD pattern of CdS nanoparticles exhibits characteristic diffraction peaks corresponding to the hexagonal (wurtzite) crystal structure, which is well matched with JCPDS card no. 41-1049. The prominent diffraction peaks are observed at 2θ values of approximately 24.8°, 26.5°, and 28.2°, indexed to the (100), (002), and (101) planes, respectively. Additional peaks appearing at around 36.6°, 43.8°, 47.9°, and 51.9° correspond to the (102), (110), (103), and (112) planes. Among these, the intense peak at ~26.5° assigned to the (002) plane confirms the preferential orientation and high crystallinity of the CdS nanoparticles, as clearly evident from the diffraction pattern.

In contrast, the CuO nanoparticles exhibit a monoclinic crystal structure consistent with JCPDS card no. 48-1548. The characteristic diffraction peaks are observed at approximately 32.5°, 35.5°, 38.7°, 48.7°, 53.5°, and 58.3°, which are indexed to the (110), (−111), (111), (−202), (020), and (202) planes, respectively. In the given pattern, the peaks around ~35.5° and ~38.7° corresponding to the (−111) and (111) planes are clearly identified, confirming the formation of CuO. These peaks are comparatively less intense than those of CdS, indicating smaller crystallite size or lower phase contribution.

For the 0.5 at% CuO–CdS nanocomposite, the XRD pattern predominantly shows the diffraction peaks of hexagonal CdS, indicating that the host lattice remains intact after CuO incorporation. In addition to the CdS peaks, weak diffraction signals corresponding to CuO are observed, particularly near ~35.5° and ~38.7°, confirming the successful loading of CuO onto the CdS matrix. The reduced intensity of CuO peaks suggests its low concentration and high dispersion within the composite. No extra impurity peaks are detected, indicating high phase purity. Furthermore, slight peak broadening in the composite pattern implies nanocrystalline nature and possible interaction between CdS and CuO, which may contribute to enhanced functional properties such as photocatalytic activity.

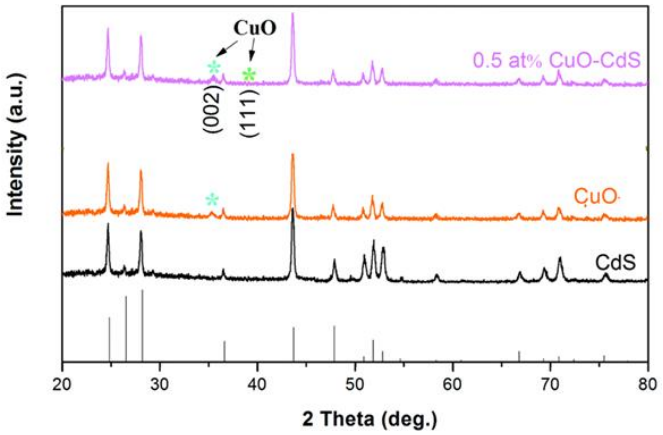

Fig. 1 XRD pattern of CuO-CdS nanocomposite

3.2 Field Emission Scanning Electron Microscope (FE-SEM) Study

The FESEM micrographs (Fig. 2) illustrate the surface morphology of (a) CuO, (b) CdS and (c) CuO–CdS nanocomposite at lower magnification, and (d) CuO–CdS nanocomposite at higher magnification. The pure CuO sample (a) exhibits agglomerated, nearly spherical nanoparticles forming dense clusters. The particles appear irregular in shape with noticeable aggregation, which is typical for chemically synthesized CuO due to high surface energy at the nanoscale. The CdS sample (b) shows comparatively finer particles with a somewhat granular morphology. Moderate agglomeration is observed, but the particle distribution appears more uniform than that of CuO. In contrast, the CuO–CdS nanocomposite (c and d) displays a distinctly modified morphology. The micrographs reveal the formation of well-defined nanostructures with flower-like and rod/needle-shaped features distributed over the surface. At higher magnification (d), the composite clearly shows elongated and interconnected nanorods embedded within clustered nanoparticles, indicating strong interfacial interaction between CuO and CdS phases.

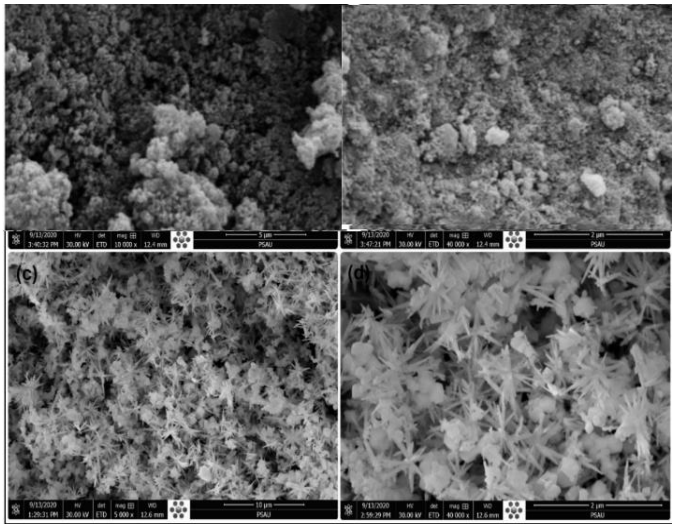

Fig. 2 FE-SEM micrographs of synthesized FE-SEM of CuO-CdS nanocomposite

https://doi.org/10.30799/jnst.S201.26110301

The transformation in morphology after composite formation suggests that CdS growth over CuO acts as a structural modifier, leading to increased surface roughness and enhanced surface area. Such hierarchical and porous structures are beneficial for photocatalytic applications as they: a) provide more active sites for adsorption of dye molecules, b) enhance light harvesting capability and c) facilitate improved charge separation and transfer.

Overall, FESEM analysis confirms successful formation of the CuO–CdS heterostructure with modified morphology compared to individual components, which is expected to contribute to enhanced photocatalytic performance.

3.3 EDAX Spectral Studies

The energy dispersive X-ray (EDX) spectrum confirms the elemental composition of the synthesized CuO–CdS nanocomposite. The prominent peaks observed in the spectrum correspond to Cu, Cd, S, and O elements, verifying the successful formation of the composite material. Fig. 3 shows the strong peaks appearing around ~0.5 keV correspond to oxygen (O), while the characteristic peaks of cadmium (Cd) are observed near ~3.1 keV. Sulfur (S) peaks appear around ~2.3 keV, confirming the presence of CdS phase. The intense copper (Cu) peaks detected at approximately ~1 keV and ~8–9 keV correspond to Cu L and Cu K transitions, respectively, indicating the presence of CuO in the composite. The absence of additional impurity peaks suggests high purity of the synthesized nanocomposite. The simultaneous presence of Cu, Cd, S, and O elements confirms the successful integration of CuO and CdS phases without contamination. The elemental composition supports the XRD and FESEM results, further validating the formation of the CuO–CdS heterostructure. The proper distribution of constituent elements is expected to facilitate efficient charge transfer across the interface, enhancing photocatalytic performance.

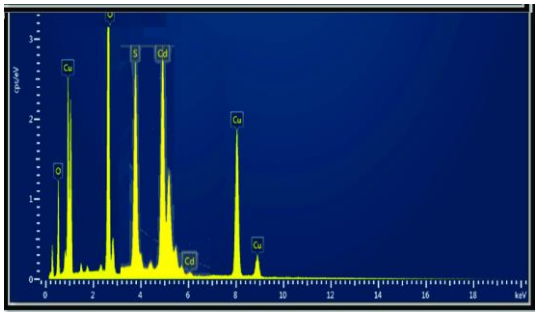

Fig. 3 EDAX spectra of synthesised CuO-CdS nanocomposite

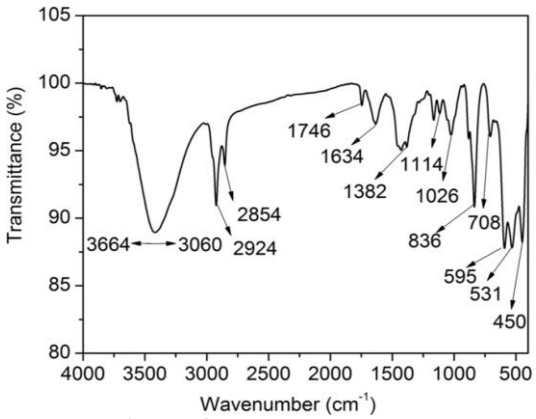

Fig. 4 FT-IR spectrum of s CuO-CdS nanocomposite

3.4 FT-IR Spectral Studies

The FTIR spectrum of the synthesized CuO–CdS nanocomposite was recorded in the range of 4000–400 cm^{-1} (Fig. 4) to identify the functional groups and confirm phase formation. A broad absorption band centered at 3664 cm^{-1} is attributed to O–H stretching vibrations of surface-adsorbed hydroxyl groups and moisture molecules. The band observed at 3060 cm^{-1} corresponds to aromatic or unsaturated C–H stretching vibrations, while the peaks at 2924 cm^{-1} and 2854 cm^{-1} are assigned to asymmetric and symmetric stretching modes of aliphatic C–H groups. These peaks may arise from residual organic species or precursor remnants from synthesis. The peak at 1746 cm^{-1} is associated with C=O stretching vibrations, possibly originating from acetate or organic precursor residues. The band at 1634 cm^{-1} corresponds to bending vibrations of adsorbed water molecules (H–O–H bending) and may also overlap with C=C stretching modes. The absorption band at 1382 cm^{-1} is attributed to C–N stretching or nitrate residues, whereas the prominent peaks at 1114 cm^{-1} and 1026 cm^{-1} correspond to C–O stretching vibrations. Importantly, the characteristic metal–oxygen and metal–sulfur vibrations are observed in the lower wavenumber region. The peak at 836 cm^{-1} can be assigned to Cd–S stretching vibrations, confirming the formation of the CdS phase. The bands at 708 cm^{-1}, 595 cm^{-1}, and 531 cm^{-1} are attributed to Cu–O stretching modes, indicating the presence of CuO. The strong absorption band at 450 cm^{-1} further confirms Cu–O lattice vibrations.

The presence of Cu–O and Cd–S characteristic bands together with the absence of additional impurity peaks confirms the successful formation of the CuO–CdS nanocomposite. The surface hydroxyl groups observed in the spectrum are expected to play a significant role in enhancing photocatalytic activity by facilitating the generation of reactive oxygen species.

3.5 UV-Vis and Photoluminescence Spectral Studies

The UV–visible absorption spectra of CuO, CdS, and the CuO/CdS nanocomposite are presented in Fig. 5(a). Pure CdS exhibits strong absorption in the UV region with a sharp absorption edge around 480–500 nm, corresponding to its characteristic band gap energy. In contrast, CuO shows broad absorption extending throughout the visible region up to approximately 800 nm, indicating its narrow band gap and strong visible light harvesting ability. The CuO/CdS nanocomposite displays a broadened absorption profile with enhanced intensity in the visible region compared to pure CdS, suggesting effective interfacial interaction between CuO and CdS and successful heterojunction formation. The slight red shift in the absorption edge further confirms improved light absorption behavior in the composite system.

The photoluminescence (PL) spectra shown in Fig. 5(b) provide insight into the charge carrier recombination behaviour. Pure CdS exhibits a strong emission peak in the range of 650–700 nm, indicating a high recombination rate of photogenerated electron–hole pairs. CuO shows relatively lower emission intensity, while the CuO/CdS nanocomposite demonstrates significant quenching of PL intensity compared to the individual components. The reduced emission intensity in the composite indicates suppressed charge carrier recombination due to efficient charge separation at the CuO/CdS interface. These results confirm that the formation of the heterojunction enhances charge transfer efficiency, which is beneficial for photocatalytic and optoelectronic applications.

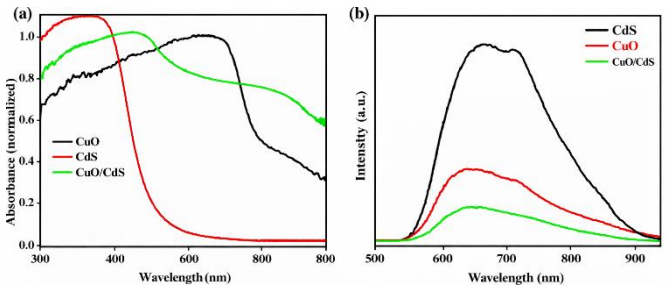

Fig. 5 a)UV–visible absorption spectra and b) photoluminescence of CuO, CdS

3.6 Photocatalytic Degradation of Methylene Blue (MB) Dye

The synthesized CuO–CdS nanocomposite was evaluated for its practical application in the photocatalytic degradation of methylene blue (MB) dye (Fig. 6), a widely used cationic dye and a common model pollutant in wastewater treatment studies. Due to its strong absorption peak at approximately 664 nm, MB serves as an ideal probe molecule for monitoring photocatalytic performance using UV–Visible spectroscopy.

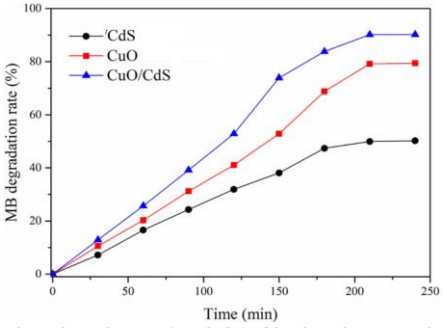

Fig. 6 photocatalytic degradation of methylene blue by CdS, CuO and CuO/CdS

Upon irradiation within the UV–Visible range (200–800 nm), the CuO–CdS heterostructure absorbs photons and generates electron–hole pairs.

https://doi.org/10.30799/jnst.S201.26110301

The formation of a heterojunction between CuO and CdS enhances charge separation efficiency and suppresses rapid recombination. The photogenerated electrons react with dissolved oxygen to produce superoxide radicals ($\bullet O_2^-$), while holes interact with water molecules or hydroxide ions to generate hydroxyl radicals (•OH). These highly reactive species are responsible for the oxidative degradation of MB dye molecules into smaller, less harmful intermediates and eventually mineralized products such as CO_2 and H_2O. The progressive decrease in the characteristic absorption intensity of MB at 664 nm confirms the effective degradation process. The enhanced visible-light absorption of the CuO–CdS composite significantly improves photocatalytic efficiency compared to individual components.

Therefore, the CuO–CdS nanocomposite demonstrates strong potential for environmental remediation, particularly in the treatment of dye-contaminated industrial wastewater. Its efficient light absorption, improved charge transfer properties, and high degradation capability make it a promising candidate for sustainable photocatalytic applications.

4. Conclusion

In the present study, a 0.5 at% CuO–CdS nanocomposite was successfully synthesized and systematically characterized using XRD, FESEM, EDAX, FT-IR, UV–visible, and photoluminescence (PL) analyses. XRD results confirmed the coexistence of hexagonal CdS and monoclinic CuO phases without the formation of secondary impurities, demonstrating successful heterostructure formation. FESEM micrographs revealed significant morphological modification in the composite compared to the individual components, showing hierarchical, flower-like, and rod-shaped nanostructures with enhanced surface roughness, which are favourable for photocatalytic reactions. EDAX analysis verified the presence of Cu, Cd, S, and O elements, confirming phase purity and proper elemental composition. FT-IR spectra further supported the formation of Cu–O and Cd–S bonds along with surface hydroxyl groups, which play a crucial role in photocatalytic activity.

Optical studies showed enhanced visible-light absorption and a slight red shift in the CuO–CdS nanocomposite compared to pure CdS. The significant quenching of PL intensity in the composite indicated efficient suppression of electron–hole recombination due to effective charge separation at the CuO/CdS interface. These improved optical and electronic properties directly contributed to enhanced photocatalytic performance. The photocatalytic degradation studies of methylene blue (MB) dye demonstrated that the CuO–CdS heterostructure exhibits superior degradation efficiency under UV–Visible irradiation. The enhanced activity is attributed to improved light harvesting, efficient charge transfer, and the generation of reactive oxygen species ($\bullet O_2^-$ and •OH) responsible for dye mineralization. Overall, the synthesized CuO–CdS nanocomposite shows excellent structural, optical, and photocatalytic properties, making it a promising candidate for environmental remediation and wastewater treatment applications.

References

[1] J.Y. Bottero, M. Auffan, J. Rose, C. Mouneyrac, C. Botta, et al., Manufactured metal and metal-oxide nanoparticles: Properties and perturbing mechanisms of their biological activity in ecosystems, C. R. Geosci. 343 (2011) 168–176.

[2] A. Rastogi, M. Zivcak, O. Sytar, H.M. Kalaji, X. He, et al., Impact of metal and metal oxide nanoparticles on plant: A critical review, Front. Chem. 5 (2017) 1–16.

[3] N. Budhiraja, Sapna, V. Kumar, M. Tomar, V. Gupta, S.K. Singh, Facile synthesis of porous CuO nanosheets as high-performance H_2S gas sensor, Integr. Ferroelectr. 193 (2018) 59–65.

[4] M.A. Gatoo, S. Naseem, M.Y. Arfat, A.M. Dar, K. Qasim, et al., Physicochemical properties of nanomaterials: Implication in associated toxic manifestations, J. Nanomater. (2014) 498420.

[5] X. Geng, P. Lu, C. Zhang, D. Lahem, M.G. Olivier, et al., Room-temperature H_2S gas sensors based on rGO@ZnO_{1-x} composites: Experiments and molecular dynamics simulation, Sens. Actuators B Chem. 282 (2019) 690–698.

[6] V.V. Burungale, R.S. Devan, S.A. Pawar, N.S. Harale, V.L. Patil, et al., Chemically synthesized PbS nanoparticulate thin films for a rapid H_2S gas sensor, Mater. Sci.-Poland 34 (2016) 204–211.

[7] F. Sarf, Metal oxide gas sensors by nanostructures, IntechOpen, London, 2019.

[8] C. Werner, P.J. Kelly, M. Doukas, T. Lopez, M. Pfeffer, et al., Degassing of CO_2, SO_2, and H_2S associated with the 2009 eruption of Redoubt volcano, Alaska, J. Volcanol. Geotherm. Res. 259 (2013) 270–284.

[9] M.R. Hoffmann, S.T. Martin, W. Choi, D.W. Bahnemann, Environmental applications of semiconductor photocatalysis, Chem. Rev. 95 (1995) 69–96.

[10] A. Fujishima, K. Honda, Electrochemical photolysis of water at a semiconductor electrode, Nature 238 (1972) 37–38.

[11] A. Kudo, Y. Miseki, Heterogeneous photocatalyst materials for water splitting, Chem. Soc. Rev. 38 (2009) 253–278.

[12] J.A. Nasir, Z.U. Rehman, S.N.A. Shah, A. Khan, I.S. Butler, C.R.A. Catlow, Recent developments and perspectives in CdS-based photocatalysts for water splitting, J. Mater. Chem. A 8 (2020) 20752–20780.

[13] Y. Bessekhouad, D. Robert, J.V. Weber, CuO nanoparticles as visible light photocatalysts, Appl. Catal. B Environ. 57 (2005) 23–29.

[14] J. Low, J. Yu, M. Jaroniec, S. Wageh, A.A. Al-Ghamdi, et al., Heterojunction photocatalysts, Adv. Mater. 29 (2017) 1601694.

https://doi.org/10.30799/jnst.S201.26110301

Cite this Article as: Gokul V. Suryawanshi, Tulshidas S. Savale, Synthesis and characterization of CuO–CdS nanocomposites for photodegradation applications, J. Nanosci. Tech. 11(3) (2026) 1078–1081.